166 (2022) 207216

Contents lists available at ScienceDirect

Micro and Nanostructures

journal homepage: www.journals.elsevier.com/micro-and-nanostructures

The radiation effects on 4H–SiC epilayers using different electron radiation methods

Bowen Yu [a], Zhao Wang [a], Yao Ma [a,b,*], Nan Yang [a], Xiaoyu Deng [a], Rui Guo [c,d], Meiju Xiang [a], Min Gong [a,b], Zhimei Yang [a,b], Yun Li [a,b], Jianer Li [e], Xueliang Li [e], Yong Feng [e]

[a] College of Physics, Sichuan University, Key Lab of Microelectronics Sichuan Province, Sichuan University, Chengdu, Sichuan, 610064, China
[b] Key Laboratory of Radiation Physics and Technology of Ministry of Education, Sichuan University, Chengdu, 610064, China
[c] School of Electronic Science & Engineering, Southeast University, Nanjing, 210096, China
[d] Nanjing Electronic Devices Institute, Nanjing, 210016, China
[e] Ritam microelectronic(Sichuan)CO., LTD, Suining, 629200, China

ARTICLE INFO

Keywords:
Silicon carbide
Electron irradiation
LOPC modes
Raman spectroscopy
X-ray diffraction

ABSTRACT

4H–SiC has a strong radiation hardness and a high breakdown voltage, making it suitable for applications in devices operating in extreme conditions; therefore, it is important to research the effects of irradiation on 4H–SiC. In this work, the effects of electron radiation on 4H–SiC under different radiation methods and fluences were studied by X-ray diffraction (XRD) and Raman spectroscopy. Changes in the FWHM in the XRD patterns under different irradiation conditions were analyzed. In the Raman spectra, changes in the FWHM in the LO phonon-plasmon coupled (LOPC) and the ratio of the intensity of the E_2 (TA) and E_2 (TO) modes were studied and discussed. Irradiation by continuous and intermittent beams led to different changes in the lattice structure and carrier characteristics.

1. Introduction

Silicon carbide is a wide band-gap (WBG) semiconductor, and 4H–SiC has a high electron saturation velocity, high thermal conductivity, and high electron mobility [1]. The complex radiation environments of space and the nuclear industry include various plasma, X-rays, and high-energy particles [2]. Solar winds consist of high-energy particles such as electrons, whose maximum energy can reach tens of MeV [3]. Electronic devices that operate in space, nuclear reactors, and other extreme conditions should be made of radiation-resistant materials. 4H–SiC is widely used in extreme conditions because of its high breakdown voltage and good radiation resistance [[4–6]]. To study the degradation performance and recover under the experimental conditions of SiC devices under test (DUTs) [[7–9]], many studies have investigated the effects of radiation on SiC epilayers; therefore, studying 4H–SiC irradiation characteristics can promote its applications in the nuclear and space fields.

Displacement damages have been observed in high-energy particles (protons, alpha particles, electrons, and neutrons) [[10,11]]. As for electron irradiation, different energies and temperatures must be considered [12]. In our previous work, we found that the body

* Corresponding author. College of Physics, Sichuan University, Key Lab of Microelectronics Sichuan Province, Sichuan University, Chengdu, Sichuan, 610064, China.
E-mail address: mayao@scu.edu.cn (Y. Ma).

https://doi.org/10.1016/j.micrna.2022.207216
Received 5 November 2021; Received in revised form 1 March 2022; Accepted 28 March 2022
Available online 5 April 2022

effect is sensitive to temperature [13] and micro-Raman measurements were used to observe partial recovery during recrystallization during annealing [14]. Raman spectroscopy and X-ray diffraction (XRD) were used to characterize these samples. The defects and crystalline states in structures were investigated by XRD measurements [15]. Harima et al. [16] used Raman spectroscopy to find the relationship between the concentration and radiation defects in SiC. Nakashima et al. [17,18] studied the simple relationship between the carrier concentration and relative Raman shift of the LOPC mode in n-type 4H–SiC with a graded donor concentration.

However, there are few studies about the effect of the irradiation methods on SiC. In this work, changes in the lattice structure and carrier characteristics under different irradiation methods (continuous and intermittent beams) and electron irradiation fluences were analyzed with XRD and Raman spectroscopy.

2. Experimental

Fig. 1 shows the 4H–SiC samples were irradiated by a 1.7 MeV electron beam using a GJ-2 high-frequency high-voltage electron accelerator (Sichuan Institute of Atomic Energy, Chengdu, China). A series of samples were irradiated in two groups. The car reciprocate with sample has same speed and different moving distance that decide the cooling time of each group and the total influence can be calculated due to the speed of car and time of duration. Group 1 was irradiated by a continuous beam (which had a small interval between irradiation), while group 2 was irradiated by an intermittent beam so it had a greater cooling time. Group 1 was irradiated at fluences of 1×10^{14} e/cm^2, 2×10^{15} e/cm^2, and 5×10^{16} e/cm^2, while group 2 was irradiated at fluences of 1×10^{14}e/cm^2, 1×10^{15} e/cm^2, and 1×10^{16} e/cm^2 at a fluence rate of 1×10^{13} e/cm^2·s. There were two samples for each fluence. It is reasonable to take one of these typical curves as the behavior at each fluence.

3. Results and discussion

3.1. XRD

Fig. 2 shows the XRD patterns of samples under different fluences in two groups. The peaks in the unirradiated sample showed a slight shift compared with other samples since it was tested at different times. In addition, double peaks were found in the XRD patterns, which may be caused by the k_β peak in the target material (Cu).

The FWHM in XRD patterns is related to crystal defects [14]. It can be concluded from Table 1 that the FWHM increased in samples at 1×10^{14} e/cm^2 in group 1 and group 2, which indicates that low-fluence irradiation may increase crystal defects. Overall, the FWHM showed a decreasing tendency upon increasing the irradiation fluence, which means that high-fluence irradiation partly decreased the defects in the crystals. In terms of the two samples in each group, the FWHM of the samples in group 2 was wider than that in group 1, indicating that there were more defects in group 1 than in group 2. Namely, thermal effects repaired more defects because the short cooling time in group 1.

It can be deduced that the different thermal effects in the two irradiation groups were caused by the different irradiation methods. Since the samples in group 1 were irradiated by a continuous beam, and the samples in group 2 were irradiated by an intermittent beam, the samples in group 1 had less cooling time. As a result, the temperature of the samples in group 1 was higher than that in group 2, so the thermal effects may have been stronger in group 1. Therefore, more cooling time in the process of radiation decreased the quality of lattice in 4H–SiC.

3.2. Raman spectroscopy

Fig. 3 shows the Raman spectra of group 1 and group 2 at different fluences. The Raman peak intensities of the two groups were

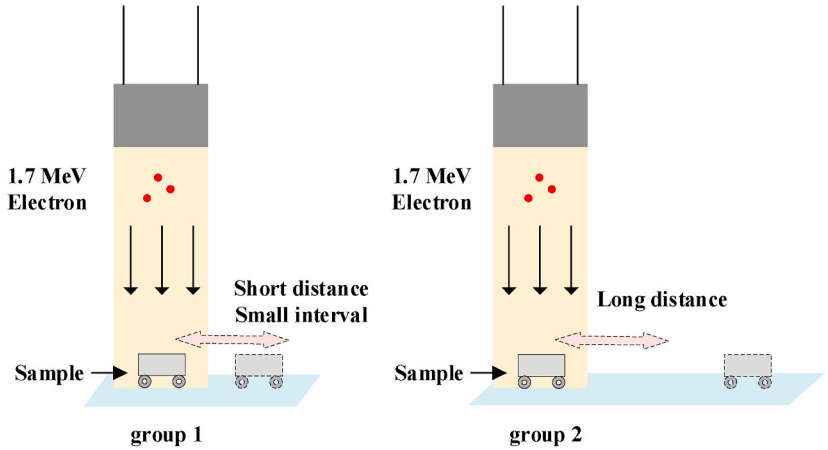

Fig. 1. The two different radiation methods.

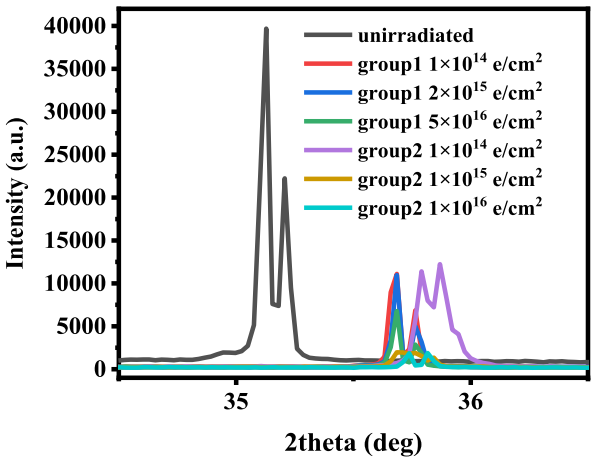

Fig. 2. XRD spectra of samples under different fluences.

Table 1
FWHM of the XRD peaks of different samples.

Group	Unirradiated sample	Group 1			Group 2		
Fluence		1×10^{14} e/cm^2	2×10^{15} e/cm^2	5×10^{16} e/cm^2	1×10^{14} e/cm^2	1×10^{15} e/cm^2	1×10^{16} e/cm^2
FWHM	0.04074	0.04239	0.035	0.0352	0.0472	0.04139	0.03599

different because they were not measured at the same time so we adjust it to almost same intensity without changing the ratio of the intensity of each peak for directly watching the difference. The following typical Raman data for 4H–SiC crystal is in the measured range [19–21]. Peaks due to the Si–Si bond vibration (TA mode at 200 cm^{-1} and TO mode at 520 cm^{-1}), the transverse optical wave of Si–C bond (794 cm^{-1}), and Si–C bond in 3C–SiC crystal (966 cm^{-1}) were observed [22]. This indicates that the experimental material was mixed with some lattice components of 3C–SiC during preparation. LOPC modes also appeared in the spectrum due to the coupling of longitudinal optical waves and free carriers in the SiC crystal. These were highly correlated with the carrier characteristics [23].

Fig. 4 shows the peak fitting (900-1100 cm^{-1}) of the Raman spectra of samples subjected to different irradiation methods and irradiation fluences. As the results in Fig. 4 show, the LOPC peak was split into two peaks at about 980 cm^{-1} and 1000 cm^{-1}, respectively. The Raman spectra of 4H–SiC were slightly different under different irradiation methods and fluences. As the results in Fig. 3 shows, in group 1 the E_2 (TA) and E_2 (TO) peaks of 4H–SiC did not change significantly, indicating that irradiation did not greatly

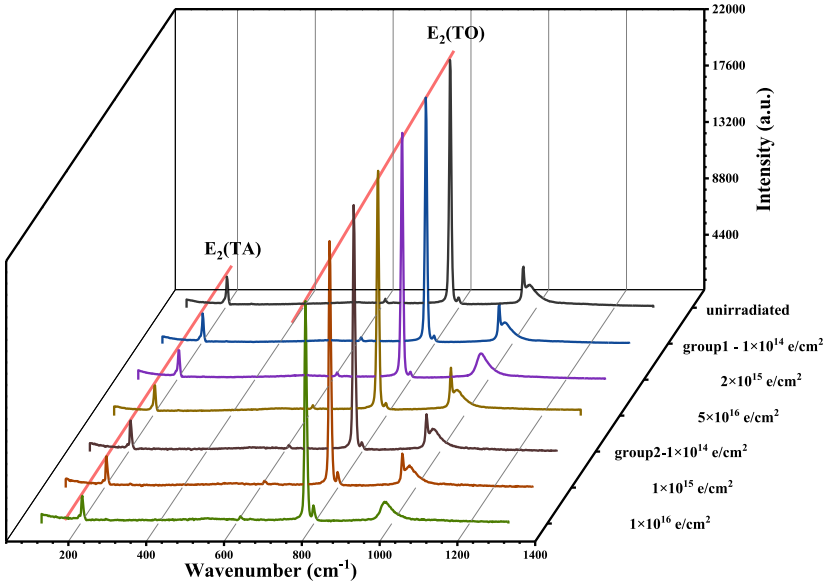

Fig. 3. Raman spectra of samples subjected to two different irradiation methods: Group 1 and Group 2.

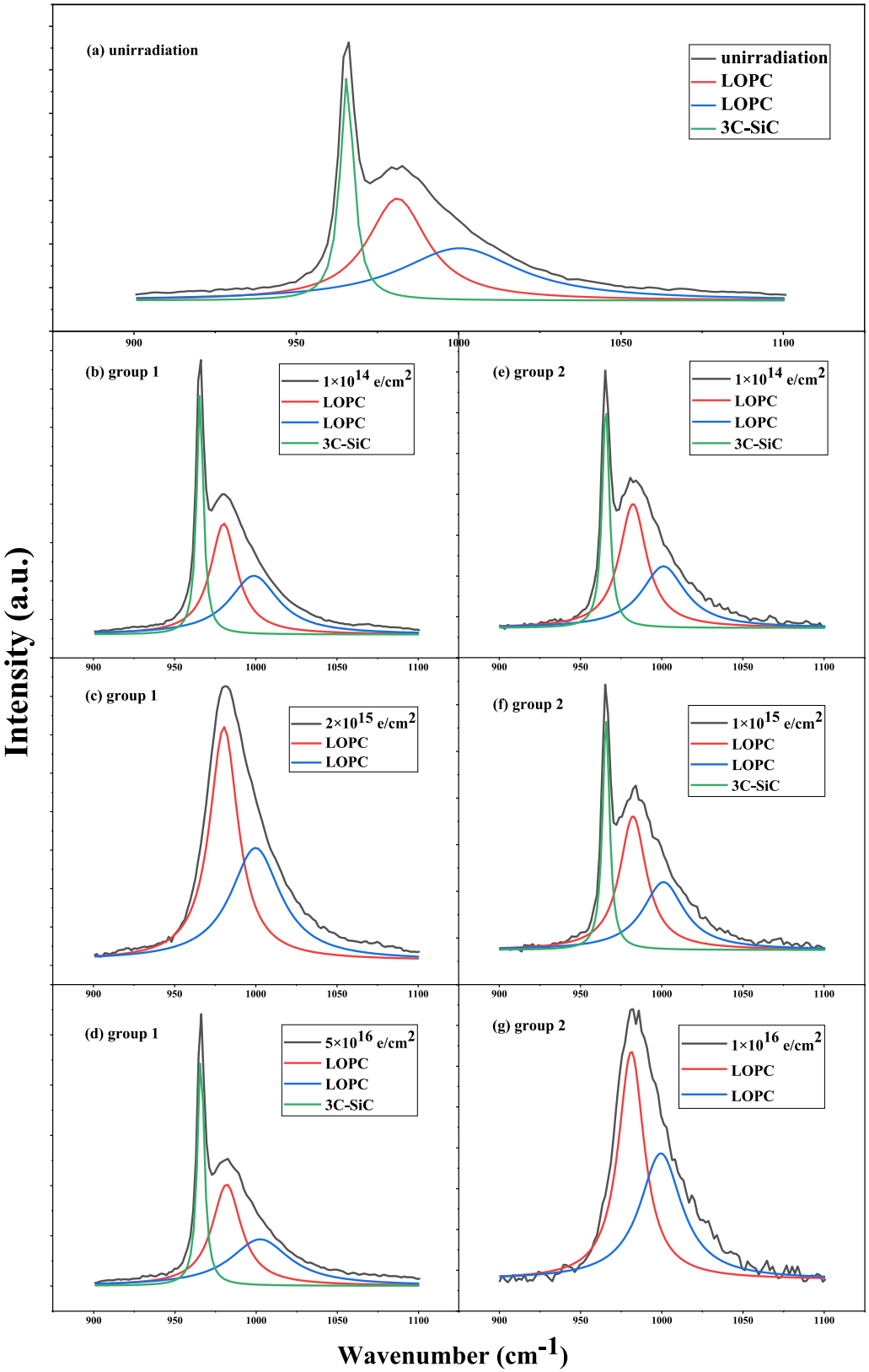

Fig. 4. Peak fitting (900-1100 cm^{-1}) of Raman spectra of samples subjected to different irradiation methods and fluences.

change the chemical bonds or lattice structure of 4H–SiC under our experimental fluences, energy, and irradiation methods. In other words, electron irradiation did not cause obvious lattice damage to the SiC lattice under our experimental conditions.

Although the SiC lattice was not obviously damaged by electron irradiation, the SiC lattice still displayed displacement damage after irradiation. By comparing the ratio of the intensity of the E_2 (TA) mode at about 200 cm^{-1} and E_2 (TO) mode at about 776 cm^{-1}, the proportion of Si–Si bonds and Si–C bonds in the SiC crystal could be qualitatively determined. Fig. 5 shows the intensity ratio of these two peaks upon changing the fluence. In group 1, as fluence increased, the ratio of the intensity of the E_2 (TO) and E_2 (TA) peak increased first and reached the maximum when the irradiation fluence was 2×10^{15} e/cm^2. As the fluence continued to increase, the ratio decreased, which means that the Si–Si and Si–C bonds also conformed to changes in the corresponding proportion of the ratio of E_2 (TO) and E_2 (TA). In group 2, the ratio of the two peaks decreased first and then increased. The ratio reached the minimum when the irradiation fluence was 1×10^{15} e/cm^2 and then reached the maximum when the irradiation fluence was 1×10^{16} e/cm^2. By comparing the ratio of E_2 (TO) and E_2 (TA) in the Raman spectra of 4H–SiC samples irradiated by the two different methods, the peak intensity ratio corresponding to these two irradiation methods showed the opposite trend to that obtained upon increasing the irradiation fluence. This may be because the temperature of the 4H–SiC epilayers in group 1 was higher than that in group 2. There was less cooling time in group 1, while group 2 had enough cooling time to compensate for the increase in temperature caused by electron irradiation effects. A higher temperature was beneficial to the annealing process because it helped recover the damaged lattice structure of 4H–SiC.

The peak position of the E_2 (TO) mode peak and FWHM showed different results upon changing the fluence under the two different irradiation methods (Fig. 6). The shift in the E_2 (TO) mode indicates changes in the elastic strain, which is caused by defects in 4H–SiC [24]. In group 1, the peak position and FWHM fluctuated upon increasing the fluence. In group 2, upon increasing the fluence, the peak position increased first, reaching the maximum at a fluence of 1×10^{15} e/cm^2, and then decreased at higher fluences. The FWHM increased with the irradiation fluence. By comparison, changes in the E_2 (TO) mode peak showed different trends under the two irradiation methods, which indicates that the effect of electron irradiation may be related to the irradiation method. In addition, the shifts of the position of the E_2 (TO) mode peak in group 2 were larger than those in group 1 at all fluences. This indicates that there were more defects in the 4H–SiC samples in group 2 than those in group 1. This also shows that the thermal effects in group 1 were stronger than those in group 2 and produced fewer defects in 4H–SiC because annealing partly reduced defects because of the higher temperature.

The insets in Fig. 3 show changes in the peaks at 966 cm^{-1} before and after irradiation. This group of peaks changed greatly, which indicates that electron irradiation greatly influenced the 3C–SiC in 4H–SiC crystals. In particular, for the two irradiation methods, the peak at 966 cm^{-1} almost disappeared at irradiation fluences of 2×10^{15} e/cm^2 and 1×10^{16} e/cm^2, respectively. It shows that the 3C–SiC component of 4H–SiC disappeared under the two irradiation fluences, corresponding to the two irradiation methods, respectively. This indicates that the 4H–SiC lattice was repaired to a certain extent under the two irradiation fluences. Fig. 7 shows changes in the FWHM and peak position of the LOPC modes. The peak at 980 cm^{-1} arose from longitudinal optical phonon-plasmon coupling originating from the interaction of free carriers with LO phonons. We obtained an empirical relationship between the carrier concentration and relative Raman shift of the LOPC mode peak [17]:

$$\omega_p^2 = \frac{4\pi n e^2}{\varepsilon_\infty m^*} \tag{1}$$

where ω_p is the plasma frequency, ε_∞ is the optical dielectric constant, m^* is the electron effective mass, γis the damping constant of the carriers, and n is the carrier concentration. We obtained the approximation ω_p^2, $(\Delta\omega)^2 \ll \omega_L^2$, ω_T^2, $(\omega_L^2 - \omega_T^2)$ for lightly-doped SiC:

$$\omega_p^2 \approx 2\omega_L(1 - \varepsilon_\infty/\varepsilon_0)^{-1}\Delta\omega \tag{2}$$

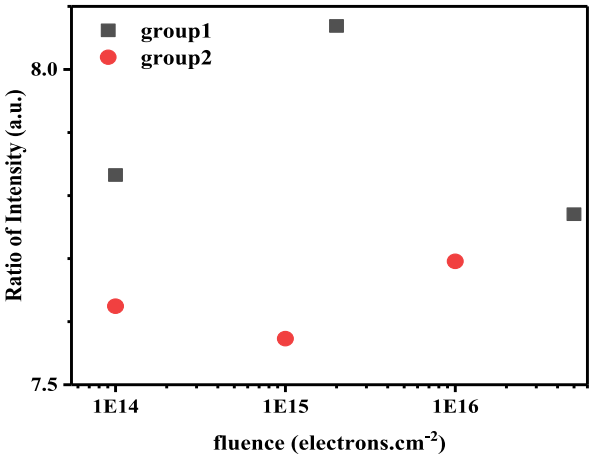

Fig. 5. The intensity ratio of the E_2 (TO) and E_2 (TA) peaks upon changing the irradiation fluence.

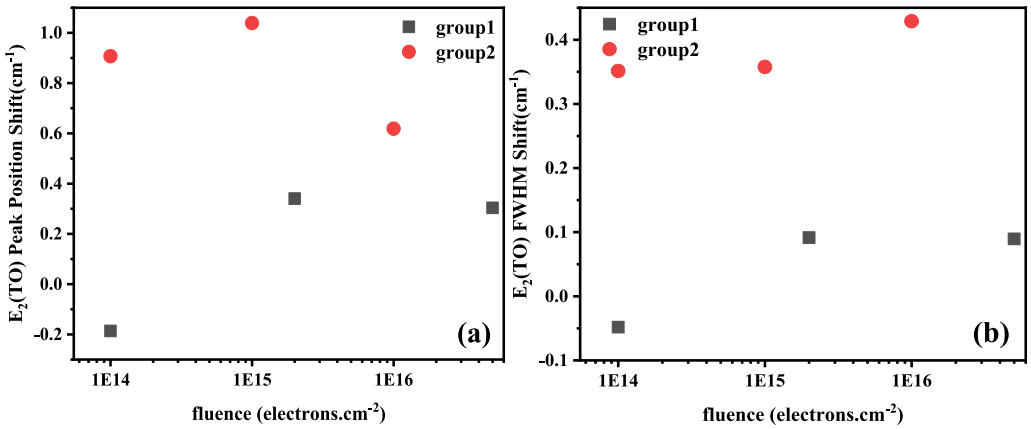

Fig. 6. Changes in the peak position and FWHM of the E_2 (TO) mode peak.

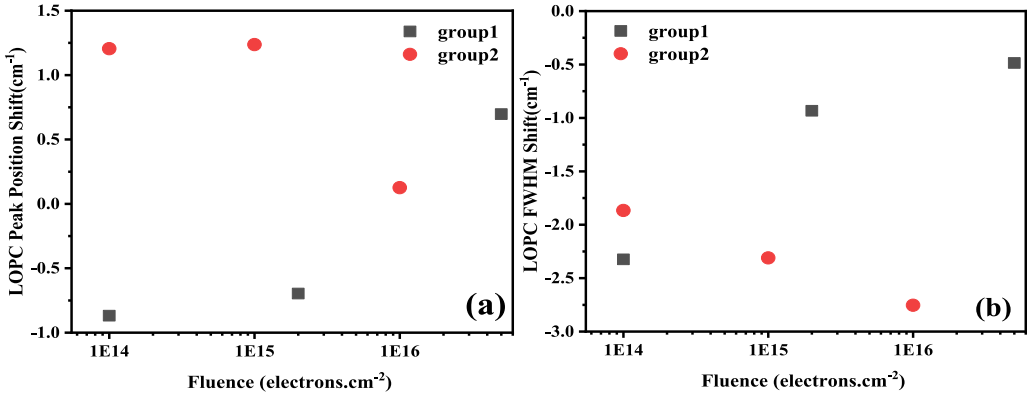

Fig. 7. The changes in the peak position (a) and FWHM of LOPC modes (b) near 980 cm^{-1}.

There is a very simple relationship between the carrier concentration and the LOPC mode frequency relative to the bare LO phonon frequency in pure 4H–SiC (cm^{-1}):

$$n = 1.25 \times 10^{17}\left(cm^{-3}\right)\left(\omega_{LOPC} - \omega_L\right)^{1.0} = 1.25 \times 10^{17}(\Delta\omega)^{1.0} \tag{3}$$

The empirical relationship in Eq. (3) is valid for the carrier-density range of 10^{17}–10^{19} cm^{-3}, where ω_L is the frequency of LO phonons, and ω_{LOPC} is the frequency of the LOPC mode.

In group 1, the peak position shift of LOPC around 980 cm^{-1} decreased first upon increasing the irradiation fluence, reaching the minimum at an irradiation influence of 1×10^{14} e/cm^2. It then increased upon increasing the irradiation fluence. This indicates that the carrier concentration in the 4H–SiC crystal decreased first and then increased with the irradiation fluence [5]. In group 2, the peak position increased first and then decreased at high fluences, and the carrier concentration in this group displayed the same trend as the peak position. Comparing the changes in the carrier concentration caused by the two irradiation methods shows that the different irradiation methods affected the carrier concentration in 4H–SiC crystals; however, these changes were very small, which indicates that 4H–SiC is strongly resistant to electron irradiation under the set fluences, regardless of whether they were irradiated continuously or pulsed.

4. Conclusion

In this study, 4H–SiC epilayers were subjected to electron irradiation with different irradiation modes (continuous and pulsed) and irradiation fluences. Changes in the crystal structure and carrier behavior of 4H–SiC before and after irradiation were analyzed by Raman spectroscopy and XRD. The XRD results showed that less cooling time in the process of radiation recovered the quality of lattice better in 4H–SiC because of the stronger thermal effects of irradiation repaired defects. Based on this, the Raman spectra showed that the crystal structure of 4H–SiC slightly changed after electron irradiation, but the composition of 3C–SiC in the 4H–SiC crystal greatly changed. There were fewer defects in 4H–SiC samples in group 1 than in group 2 and at the same time, the carrier concentration changed slightly upon changing the electron irradiation fluence, and it changed differently in the two groups because of the different effects of continuous beams and intermittent beams. Further work is needed to use radiation hardened by design (RHBD) to optimize

the SiC device for the thermal effects because electronics operating in space experience many different radiation modes, including intermittent and continuous beams. The device will be damaged more severely if it worked in the intermittent radiation beams which has long cooling time to compensate for the increase in temperature caused by electron irradiation effects.

Author statement

Bowen Yu: Conceptualization, Methodology, Software, Investigation, Formal analysis, Visualization, Writing – original draft. **Zhao Wang**: Software, Investigation, Formal analysis, Writing – original draft. **Yao Ma**: Conceptualization, Funding acquisition, Resources, Supervision, Writing – review & editing. Nan Yang: Data curation, Formal analysis. **Xiaoyu Deng**: Data curation, Formal analysis. **Rui Guo**: Conceptualization, Software. **Meiju Xiang**: Conceptualization, Software. **Min Gong**: Conceptualization, Writing – review & editing. **Zhimei Yang**: Resources, Validation. **Yun Li**: Resources, Validation. **Jianer Li**: Resources **Xueliang Li**: Resources Yong Feng: Resources.

Declaration of competing interest

The authors declare that they have no known competing financial interests or personal relationships that could have appeared to influence the work reported in this paper.

Acknowledgements

This paper was supported by the fund of the Innovation Center of Radiation Application under Grant No. KFZC2020021001, the National Natural Science Foundation of China under Grant No. 61704116 and 11875068, and the Science and Technology on Analog Integrated Circuit Laboratory under Grant No. 6142802190505.

References

[1] Heyi Li, et al., Irradiation effect of primary knock-on atoms on conductivity compensation in N-type 4H-SiC Schottky diode under various irradiations, Semicond. Sci. Technol. 34 (9) (2019), 95010.
[2] J Ford. Radiation, people and the environment, International Atomic Energy Agency (IAEA), 2004.
[3] J. Barth, Natural Radiation Environment Definition for Electronic System Design, 2002, p. GOMAC2002.
[4] J.A. Cooper Jr., A.K. Agarwal, SiC power-switching devices - The second lectronics revolution?", Proc. IEEE 90 (No. 6) (2002) 956–968.
[5] A.T. Paradzah, F.D. Auret, M.J. Legodi, E. Omotoso, M. Diale, Electrical characterization of 5.4 MeV alpha-particle irradiated 4H-SiC with low doping density, Nucl. Instrum. Methods Phys. Res. Sect. B Beam Interact. Mater. Atoms 358 (2015) 112–116.
[6] D.J. Brink, J.B. Malherbe, J. Camassel, Neutron irradiation effects in SiC, Nucl. Instrum. Methods Phys. Res. Sect. B Beam Interact. Mater. Atoms 267 (2009) 2716–2718.
[7] S. Sorieul, et al., Optical spectroscopy study of damage induced in 4H-SiC by swift heavy ion irradiation, J. Phys. Condens. Matter 24 (12) (2012) 125801.
[8] Indudhar Panduranga Vali, et al., Structural and optical studies of gamma irradiated N-doped 4H-SiC, Nucl. Instrum. Methods Phys. Res. Sect. B Beam Interact. Mater. Atoms 440 (2019) 101–106.
[9] Zhimei Yang, et al., XTEM investigation of recovery on electrical degradation of 4H-SiC Schottky barrier diode by swift heavy 209Bi ions irradiation, Nucl. Instrum. Methods Phys. Res. Sect. B Beam Interact. Mater. Atoms 407 (2017) 304–309.
[10] Pavel Hazdra, Stanislav Popelka, Displacement damage and total ionisation dose effects on 4H-SiC power devices, IET Power Electron. 12 (15) (2019) 3910–3918.
[11] Yitao Yang, et al., Damage and recovery behavior of 4H-SiC implanted with Heions, Nucl. Instrum. Methods Phys. Res. Sect. B Beam Interact. Mater. Atoms 449 (2019) 54–57.
[12] Pavel Hazdra, Vobecký Jan, Radiation defects created in n-type 4H-SiC byElectron irradiation in the energy range of 1–10 MeV, Phys. Status Solidi 216 (17) (2019) 1900312.
[13] D. Wang, et al., Heavy ion radiation and temperature effects on SiC Schottky barrier diode, Nucl. Instrum. Methods Phys. Res. Sect. B Beam Interact. Mater. Atoms 491 (6) (2021) 52–58.
[14] M. Huang, et al., Recrystallization effects in GeV Bi ion implanted 4H-SiC Schottky barrier diode investigated by cross-sectional Micro-Raman spectroscopy, Nucl. Instrum. Methods Phys. Res. Sect. B Beam Interact. Mater. Atoms 478 (11) (2020) 5–10.
[15] T. Sawabe, et al., Estimation of neutron-irradiation-induced defect in 3C–SiC from change in XRD peak shift and DFT study, J. Nucl. Mater. 417 (2011) 1–3.
[16] A. Mjm, et al., Characterization of 167MeV Xe ion irradiated n-type 4H-SiC, Appl. Surf. Sci. 493 (2019) 1291–1298.
[17] S. Nakashima, et al., Raman scattering study of carrier-transport and phonon properties of 4H-SiC crystals with graded doping, Phys. Rev. B 76 (24) (2007) 4692.
[18] S. Nakashima, H. Harima, Raman investigation of SiC polytypes, Physica Status Solidi Applied Research 162 (1) (2015) 39–64.
[19] J.C. Burton, et al., Spatial characterization of doped SiC wafers by Raman spectroscopy, J. Appl. Phys. 84 (11) (1998) 6268–6273.
[20] J.C. Burton, et al., First-and second-order Raman scattering from semi-insulating 4 H– SiC, Phys. Rev. B 59 (11) (1999) 7282.
[21] S.-I. Nakashima, H. Harima, Raman investigation of SiC polytypes, Phys. Status Solidi 162 (1) (1997) 39–64.
[22] Yi Han, et al., H-ion irradiation-induced annealing in He-ion implanted 4H-SiC, Chin. Phys. Lett. 34 (1) (2017), 12801.
[23] Moshawe J. Madito, et al., Characterization of 167 MeV Xe ion irradiated n-type 4H-SiC, Appl. Surf. Sci. 493 (2019) 1291–1298.
[24] Takaaki Koyanagi, Yutai Katoh, J. Michael, Lance, Raman spectroscopy of neutron irradiated silicon carbide: correlation among Raman spectra, swelling, and irradiation temperature, J. Raman Spectrosc. 49 (10) (2018) 1686–1692.